



Characterization and evaluation of curcumin loaded guar gum-polyhydroxyalkanoates blend film for wound healing application

Journal:	<i>RSC Advances</i>
Manuscript ID:	RA-ART-05-2015-010114.R1
Article Type:	Paper
Date Submitted by the Author:	06-Jul-2015
Complete List of Authors:	Pramanik, Nilkamal; University of Calcutta, Mitra, Tapas; University of Calcutta, Khamrai, Moumita; University of Calcutta, Bhattacharyya, Aditi; University of Calcutta, Mukhopadhyay, Piyasi; University of Calcutta, Gnanamani, A; CLRI, Basu, Ranjan; University of Calcutta, Kundu, Patit; CU, Polymer Science & tech



Journal Name

ARTICLE

Characterization and evaluation of curcumin loaded guar gum-polyhydroxyalkanoates blend film for wound healing application

Received 00th January 20xx,
Accepted 00th January 20xx

DOI: 10.1039/x0xx00000x

www.rsc.org/

Nilkamal Pramanik¹, Tapas Mitra¹, Moumita Khamrai¹, Aditi Bhattacharyya¹, Piyasi Mukhopadhyay¹, A. Gnanamani², Ranjan Kumar Basu³, Patit Paban Kundu^{1*}

The present paper explores the *'insitu'* fabrication of guar gum-polyhydroxyalkanoates-curcumin blend (GPCC) films in view of their increasing applications as wound dressing and antibacterial materials. Curcumin is incorporated to assess its bactericidal activity and enhance production and accumulation of extracellular matrix in the healing process. In order to characterize the nature of polymer network in the blend, ATR-FTIR spectra and TGA analyses are performed. The results reveal that the rigidity of guar gum-PHBV blend improves with the increment of the PHBV content due to the formation of non-covalent interaction especially H-bonds between these molecules. Electron microscopy analyses reveal the homogeneity of blends and surface roughness of the blended films, favoring the cell attachment and cell proliferation compared with the film without curcumin. The anti-microbial study demonstrates that the bactericidal activity is more effective against gram-positive strains than that of gram-negative strains. Results of the *invivo* wound healing study in animal model demonstrate that the developed curcumin loaded guar gum-PHBV blend film shows markedly enhanced wound healing compared to the control one.

Introduction

In recent years, the bioplastics like polyhydroxyalkanoates (PHA) having biodegradable and bio-compatible properties^{[1-}

^{3]} have shown great potential as an alternative of petroleum based plastics. Typically, such biomaterials having excellent pore-interconnectivity, biodegradable and biocompatible properties appear to be a suitable substrate to enable cell

adhesion, migration, proliferation and differentiated function on disrupted tissues^[4-5]. The mode of application of such biomaterials in biomedical devices as surgical sutures, regenerative tissues, multi-receptor vehicles etc is the promising tool for today's remedial outcomes^[6-10].

In the biomedical field, the biocompatible assays of different polymers such as poly(3-hydroxybutyrate) (PHB), poly(3-hydroxybutyrate-co-3-hydroxyvalerate) (PHBV) etc show good biocompatibility to various cell lines, including osteoblastic, epithelial cell and ovine chondrocytes^[11-12]. The biocompatibility and cell proliferation mainly depend on the permeability of the material through the cell membrane^[13]. In this aspect, the hydrophobic PHA can easily penetrate into the hydrophobic channel of cell. Therefore, the transfer of salts across the hydrophobic barriers is accelerated, resulting in a potential physiological niche for PHB in cell metabolism^[14].

Different biomedical applications like wound dressing, surgical mesh, adhesion barriers, bone plates etc depend on the physical and mechanical properties of the biomaterials. Polyhydroxyalkanoates are well known biodegradable materials but hydrophobicity and brittleness^[15] hinder its rate of swelling and flexibility. Therefore, the biopolymer like PHA needs to be modified by the blending with another polymers or modifying it with inorganic materials, improving their physical, mechanical properties and biocompatible properties^[16]. Investigation on blends of polyhydroxyalkanoates with naturally occurring hydrophilic biopolymers has attracted much interest in the recent years. Blends of polyhydroxyalkanoates with another biopolymers e,

g. chitosan, polyvinyl alcohol has been already reported as wound dressing or scaffold materials^[15-17].

Recently, wound healing is found to be a part of most clinical trial in the tissue engineering^[18], but the proper way of treatment with the interdependent and overlapping phases^[19] such as -a) haemostasis, b) Inflammatory phase, c) Migratory phase, d) Proliferative phase and e) Remodelling phase, is not only complex but fragile and exist in a steady-state equilibrium, forming a protective barrier against the external environment. Once the protective barrier is broken, the normal (physiologic) process of wound healing is immediately set in motion. Many researchers have already reported the promising tool for wound healing in which polyhydroxyalkanoates (hydrophobic component) were used to improve the proliferation of cells^[20, 21] during wound healing. But, both hydrophobic and hydrophilic action required for cell proliferation during wound healing cannot be achieved by a single biopolymer^[20, 22].

Therefore, researchers are more prone to set up a hydrophilic-hydrophobic conjugated wound dressing biomaterial to promote the wound healing process. Murakami et al^[23], Kil'deeva^[24] et al and Zhijiang et al^[25] explained in their experimental analysis that the cell proliferation and biocompatibility assays on PHA blended composite film exhibited better performance than that of the pure polyhydroxyalkanoate based film during wound healing processes.

Guar gum is a high-molecular weight water-soluble non-ionic natural polysaccharide. The backbone is a linear chain of β -1, 4-linked mannose residues to which galactose residues are 1,

6-linked at every second mannose, forming short side-branches. Due to its hydrophilicity, biodegradability and biocompatibility, guar gum is extensively used in the field of biotechnology as bio-absorbable materials for wound healing [26]. Guar gum is one of the most promising dietary fibre, easily soluble in cold water and has high viscosity at low concentration. Each of guar gum having a considerable number of hydroxyl groups in outer sphere together with the simultaneous presence of hydrophobic regions in their structure may reinforce the interactions with both non-ionic and ionic drugs [27].

The incorporated drug, curcumin (diferuloylmethane, a polyphenol) is a bioactive agent of the perennial herb *Curcuma longa* (commonly known as turmeric). It is a naturally occurring polyphenolic phyto constituent which plays vital role in anticancer, antibacterial, and wound healing activities.

Therefore, in the present study, we have investigated the blends of hydrophobic polyhydroxyalkanoates and hydrophilic guar gum as a potential vehicle for release of wound healing material, curcumin. Again, it also deals with the preparation of biocomposite film to protect UV-rays and also to facilitate the cell adhesion onto the porous material with the sustainable release of drug in wound healing steps.

Results

Thickness of guar gum/ PHBV composite films

The guar gum/PHBV blend (GPC) films were fabricated using solvent casting method. The thickness of the blend films with various ratios, [7:3, 5:5 and 3:7] of guar gum and PHBV was measured to be $0.57 \pm 45 \mu\text{m}$.

Mechanical properties

Table 1 displayed the relationship between the tensile strength and PHBV content in the blend. 30% PHBV content in guar gum-PHBV blend exhibited a maximum strength (about 19.8 MPa) compared to pure guar gum (16.3 MPa). Again, the tensile strength of guar gum/PHBV blend showed the decreasing trend from 19.8 MPa to 8.3 MPa with the increase in PHBV content from 30% to 70%.

Table 1. Effect of poly (3hydroxybutyrate-co-3hydroxyvalerate) copolymer on tensile strength and elongation at break of Guar gum film.

Sample	Tensile Strength (MPa)	Elongation at break (%)	Modulus (MPa)
Pure guar gum	16.3±0.57	60.11	23
Guar gum/PHBV (7:3)	19.8±0.77	72.96	9.23
Guar gum/PHBV(5:5)	12.2±0.77	49.2	5.64
Guar gum/PHBV (3:7)	8.3±0.57	39.29	15.2
Pure PHBV	4.2±0.77	34.6	159

Optical properties

Figure 1 showed that the absorbance of UV-Visible light is maximum for 70% PHBV content in the blend film compared to the pure guar gum film. Again, the opacity of pure guar gum and guar gum/PHBV blend films followed the same order as their absorbance while the transparencies were completely reversed to absorbance as shown in **Table 2**.

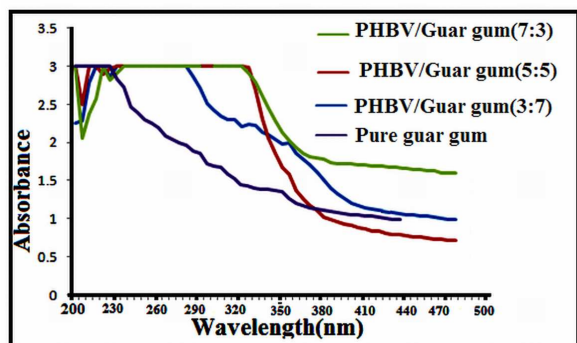


Figure 1: Optical behavior (UV-Visible light absorption) of Guar gum and prepared composite films with various ratios of PHBV and guar gum.

Table 2. Effect of poly (3hydroxybutyrate-co-3hydroxyvalerate) on opacity and transparency of guar gum/PHBV composite films

Sample	Opacity of specimens	Transparency
Pure guar gum	35.69±0.77	28.9±0.57
Guar gum/PHBV (7:3)	44.055±0.77	24.5±0.77
Guar gum/PHBV (5:5)	76.95±0.577	22±0.57
Guar gum/PHBV (3:7)	80.55±0.577	12.4±0.77

Proton nuclear magnetic resonance (^1H NMR) spectral analysis

^1H NMR spectra of isolated pure curcumin, guar gum and poly(3hydroxybutyrate-co-3hydroxyvalerate) was shown in **Figure 2**. Pure curcumin showed the strong resonance peaks at $\delta_1=3.798$ ppm, $\delta_2=3.882-3.904$ ppm, $\delta_3=5.735$ ppm, $\delta_4=6.77-6.852$ ppm, $\delta_5=7.0-7.2$ ppm and $\delta_6=7.55$ ppm. On the other hand, poly(3hydroxybutyrate-co-3hydroxyvalerate) copolymer exhibited chemical shift (δ) values at $\delta_7=0.874$

ppm, $\delta_8=1.256$ ppm, $\delta_9=1.599$ ppm, $\delta_{10}=2.016$ ppm, $\delta_{11}=2.31$ ppm and $\delta_{12}=5.339$ ppm respectively. Again, peaks at $\delta_{13}=5.0$ ppm, $\delta_{14}=4.72$ ppm, $\delta_{15}=3.5$ ppm, $\delta_{16}=3.7$ ppm, $\delta_{17}=3.8(d)-3.9(d)$ ppm, $\delta_{18}=4.1(s)-3.95(s)$ ppm respectively assigned the equatorial and axial protons in guar gum molecule.

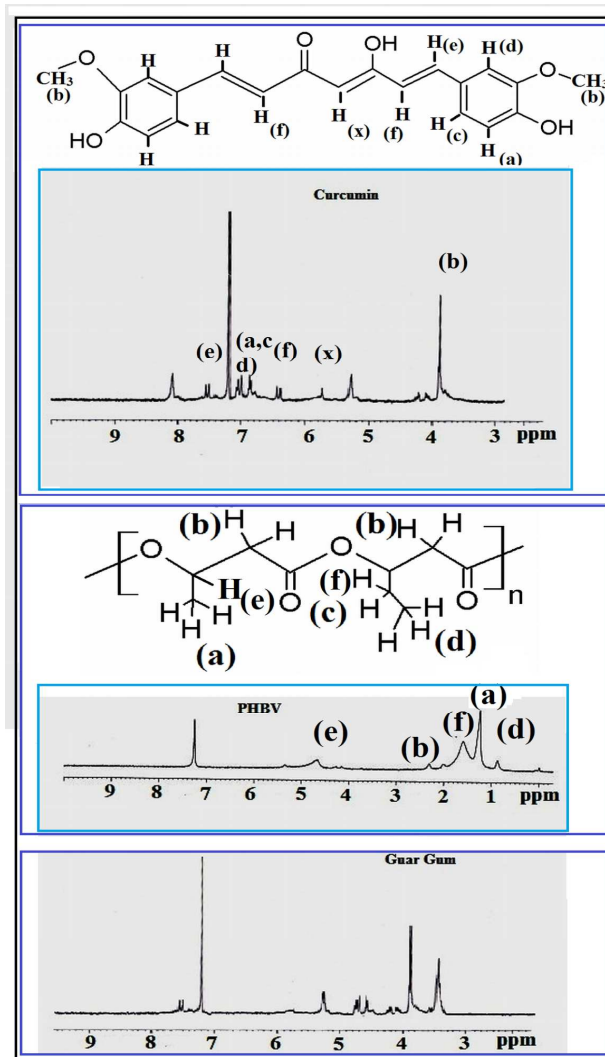


Figure 2: ^1H NMR spectra of pure PHBV, pure guar gum and curcumin.

Fourier transform infrared spectroscopic (FTIR) analysis

Figure 3 demonstrated the profile of stretching frequency of PHBV polymer and its guar-gum/PHBV blend films. The stretching frequency of different C-C, C-O, C=O, C-H, C-

OOR groups of the corresponding compounds and their blend showed in [ESI 1 Table 3].

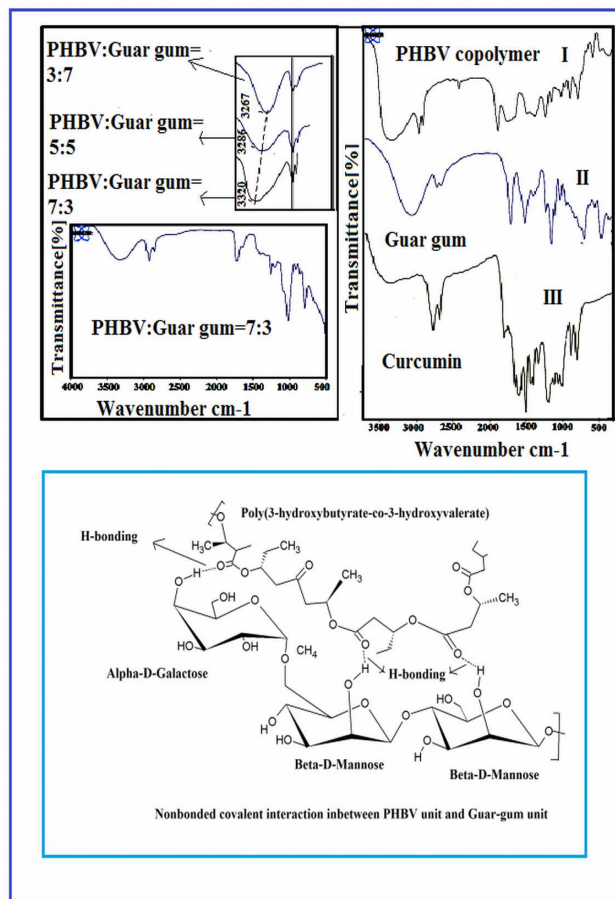


Figure 3: FT-IR/ ATR spectra of pure PHBV, Guar gum and prepared composite films with various ratios of PHBV and guar gum.

Pure guar gum and PHBV showed the main absorption peaks at 11048, 1275, 1386.63, 1452.29, 1639.7, 1726, 1576.86, 2880.65, 2934 and 3268 and 3469.27 cm^{-1} , respectively. Again, pure curcumin absorbs the energy in term of wave number in the following regions: 725, 814, 1123, 1512, 1624, 1741, 2851-2923.52 and 3410 cm^{-1} due to the presence of aromatic and aliphatic bending and stretching of C-H group

and enolic -OH group, respectively. For guar gum/PHBV blend film, the -C=O stretching frequency of PHBV was found to decrease from 1726 cm^{-1} to 1721 cm^{-1} and the strong absorption frequency was also found to shift to higher values with the increasing contents of PHBV in the film [Fig 2 and ESI 1 Table 3].

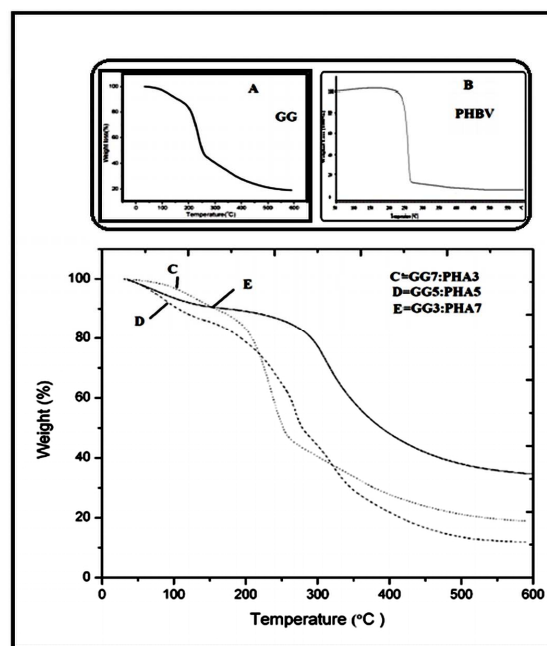


Figure 4: Thermo gravimetric analysis of A) pure guar gum, B) PHBV, C) guar gum/PHBV (7:3), D) guar gum/PHBV (5:5) and E) guar gum/PHBV (3:7) composite.

Thermo gravimetric (TGA) analysis

Thermal degradation of guar gum, PHBV and their blend were conducted using a TGA Q 50(V20.6 build 31) instrument as shown in **Figure 4**. The results indicated about the two steps degradation, primarily in temperature ranges of 60-100°C and in the second step in ranges of 150-330°C. For both of guar gum and PHBV, initially, the respective minimum weight loss of 8% and 5% was observed at 120°C and it was found to shift to the maximum values of 52% and

ARTICLE

Journal Name

33% at an enhanced thermal point of 250°C as shown in **Table 4**. But, in case of guar gum/PHBV blends [7:3, 5:5, 3:7], the rate of molecular degradation was found to be retarded initially and only 68%, 62% and 33% of weight loss were recorded in the temperature ranges of 200 to 400°C.

Table 4. First and second decomposition temperatures and percentage of total weight loss for various Guar gum, PHBV and Guar gum/PHBV polymeric composite films.

Sample	Initial Weight Loss	Weight Loss (%)	Intermediate Weight Loss	Weight Loss (%)	Total Weight Loss (%)
	Temperature (°C)		Temperature (°C)		
Guar gum	74	1.2	260	56	57.2
PHBV	210	7	250	33	40
GG /PHBV (7:3)	126	12	284, 411	52, 80	64, 92
GG /PHBV (5:5)	146	8	275	68	76
GG /PHBV (3:7)	151	10	251, 350	33, 60	43, 70

Differential scanning calorimetric (DSC) analysis

The melting temperature of the blend was determined through the DSC thermogram analysis (temperature range of 30 to 200°C at the rate of 10°C/ min). It reveals two endothermic melting peaks at 164°C and 174°C. The melting peak at 174°C is due to the presence of incorporated curcumin molecule [28].

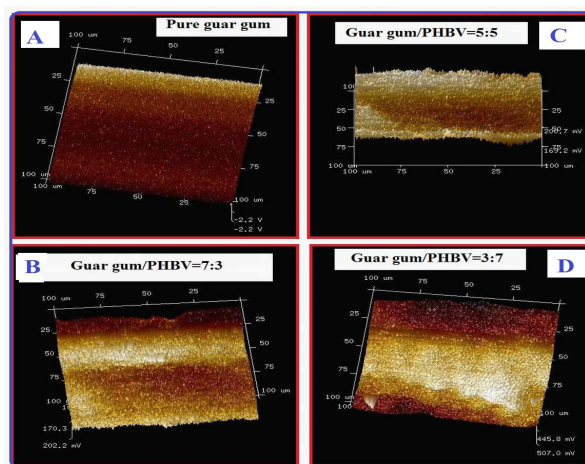


Figure 5: AFM images of pure guar gum (A) and prepared composite films with various ratios of PHBV and guar gum. [B] Guar gum/PHBV (7:3), C) Guar gum/PHBV (5:5) and Guar gum/PHBV (3:7)].

Atomic force microscopic (AFM) analysis

In order to investigate the influence of guar gum and PHBV biopolymer on the surface properties of the membrane, atomic force microscopic (AFM) experiments [AFM ((VEECO, Multimode Nanoscope IIIa))] operating in tapping mode (RTESP Tip with resonant frequency of 301.78 KHz) at room temperature were performed. **Figure 5** exhibited the images of three-dimensional 20 μm scans for pure guar gum and its PHBV blend films. The pure guar gum film showed comparatively favorable uniform and smooth surface than guar gum/PHBV blend films. The surface appearance for pure guar gum film dealt with the homogeneous morphology and distribution features. The roughness (RMS) on to the surface was found to increase in a consecutive way [8.4 nm, 16.4 nm, 26.5 nm and 32 nm] with an increasing content of PHBV with more irregularities and some new protuberances and unevenly distributed features were also observed.

Swelling study

Figure 6 depicted the swelling kinetics of pure guar gum and its PHBV blend films. The pure guar film showed a swelling of 442% in physiological saline solution at pH 7.4. The highest percentage (472%) of swelling was observed for blend film at 30% of PHBV while the blend films with 50% and 70% of PHBV exhibited a decrease in equilibrium swelling from 320% to 200%.

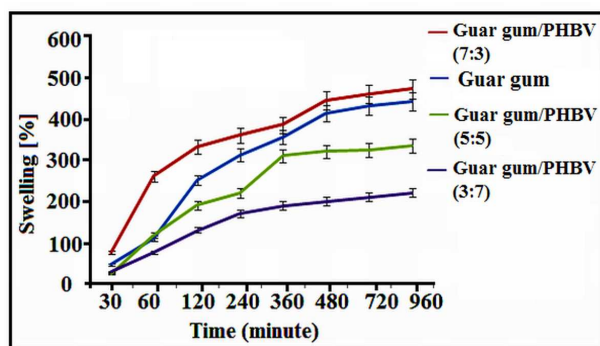


Figure 6: Swelling capacity of PHBV/guar gum blend and pure guar gum films. (A) 3:7 (B) 5:5 and (C) 7:3 ratio of PHBV and guar gum.

Etching study

Etching of different guar gum/PHBV films was conducted to realize the homogeneity of two components in the blend films by observing the etched surface under scanning electron microscope. **Figure 7** showed that with the increasing content of PHBV, the surface roughness increased and porosity was well distributed throughout the surface of the film.

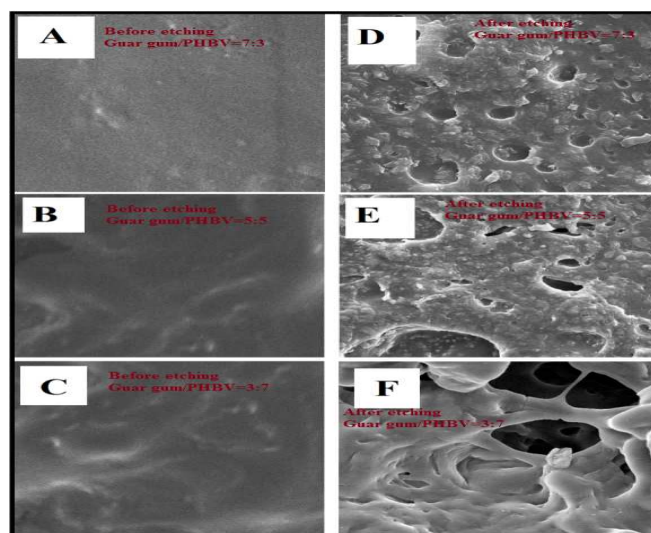


Figure 7: SEM images of surface morphology of different ratios of PHBV/guar gum blend film before etching [(A) 7:3, (B) 5:5 and (C) 3:7] and after etching [(D) 7:3, (E) 5:5 and (F) 3:7].

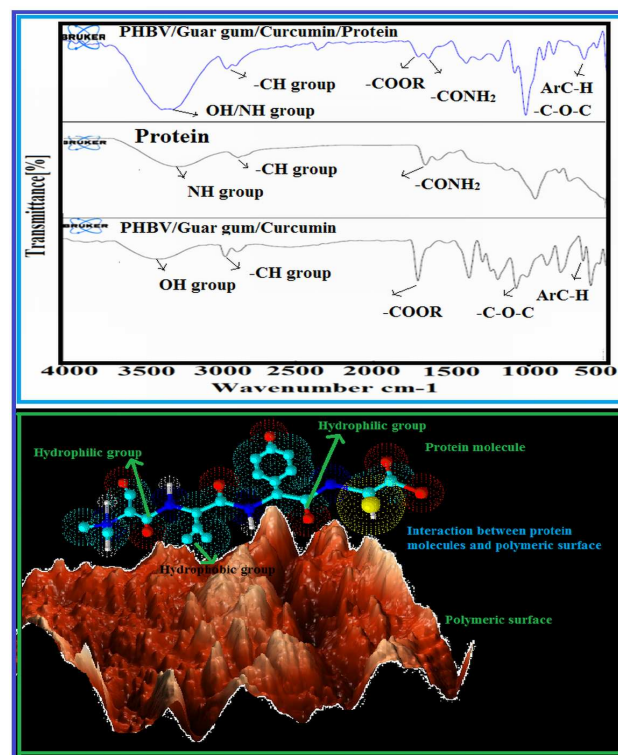


Figure 8: ATR-FTIR spectra of PHBV/Guar gum/ curcumin-BSA adsorbed blend film.

Protein adsorption study

Protein adsorption onto the surface of polymeric films indicated the increasing order of BSA (Bovine Serum Albumin) content with an increase in the hydrophobicity in blend films. The BSA adsorption onto the pure guar-gum film was found to be nearly 37%. But, in case of modified guar gum/PHBV and guar gum/PHBV/curcumin blend film, the adsorption amount was augmented to 64% and 70% respectively. Again, the ATR spectral analysis [Figure 8] of BSA adsorbed guar gum/PHBV/curcumin blend film showed the intense absorption peaks at 3400 cm^{-1} , 3100 cm^{-1} , $1600\text{--}1700\text{ cm}^{-1}$, 1510 and 1580 cm^{-1} region.

Hemolytic assays

Figure 9 indicated the relevance of blood-compatibility of the blend film. A low percentage (4%) of blood cell hemolysis was observed with the test sample in comparison to the negative test. But, in case of positive test, the cell membrane of hemoglobin was found to be completely damaged in distilled water. The blood compatibility efficiency and hemolytic activity of the specimen is comparable to the previous report [29].

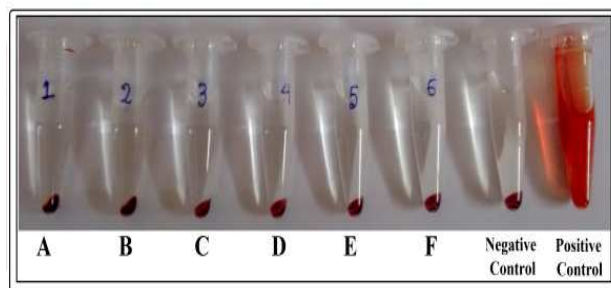


Figure 9: Hemolytic assays of the PHBV/guar gum/curcumin loaded composite film. [A-10 $\mu\text{g/ml}$, B-20 $\mu\text{g/ml}$, C-30 $\mu\text{g/ml}$, D-40 $\mu\text{g/ml}$, E-50 $\mu\text{g/ml}$, F- 100 $\mu\text{g/ml}$, Negative control (PBS solution) and Positive control (water)].

Antimicrobial activity

Figure 10 displayed the inhibition of bacterial cell against several microorganisms in the presence of pure curcumin and curcumin loaded film. Curcumin and curcumin loaded films exhibited a significant activity against gram-positive strains compared to gram-negative strains. Curcumin and its blend film exhibited around 17.5 ± 0.57 mm zone of inhibition in gram-positive strains and $15\text{--}14 \pm 0.77$ mm of inhibition in gram-negative strains. This reported value is in agreement with the report previously described by Negi et al [30].

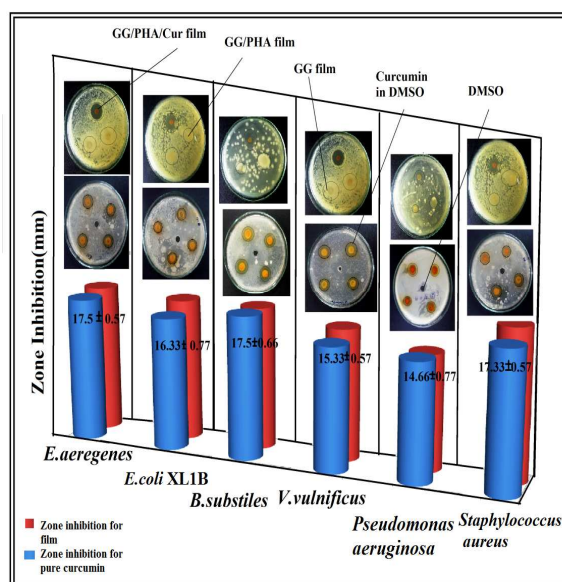


Figure 10: Antibacterial activity of prepared composite films against several gram-positive and gram-negative bacteria strains (a) pure curcumin and (b) curcumin composite films.

In vitro drug release study

The *in vitro* drug release behavior of different guar gum/PHBV blend films were studied and reported in Figure 11. This figure indicated that the release of curcumin from curcumin loaded guar gum/PHBV blend films occurred in a controlled manner. It was noticeable that the rate of drug release was decreased with the increasing content of PHBV

into the film composition. Since, a burst release (95.14%) of curcumin was observed from pure guar gum film, while 70% of PHBV content film displayed sustained release (62.86%) of curcumin in 36 hours.

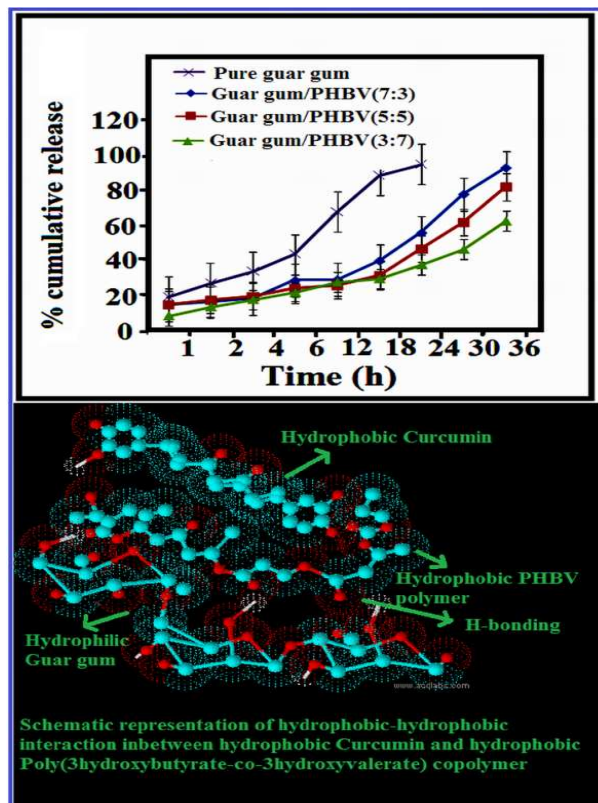


Figure 11: *In vitro* release profile of curcumin from PHBV/guar gum/curcumin loaded composite film in PBS at pH 7.4.

Cell viability

The general morphology of the fibroblast NIH 3T3 cells was incubated with pure guar gum and its PHBV/curcumin blend was monitored in a phase-contrast microscope. For native curcumin and guar gum, 4 mg/ml was found to be optimum with high cell viability (85%) as shown in **Figure 12**. Comparable inhibition of cell proliferation was observed for guar gum/PHBV blend and guar gum/PHBV/curcumin blend with 75-80% of cell viability.

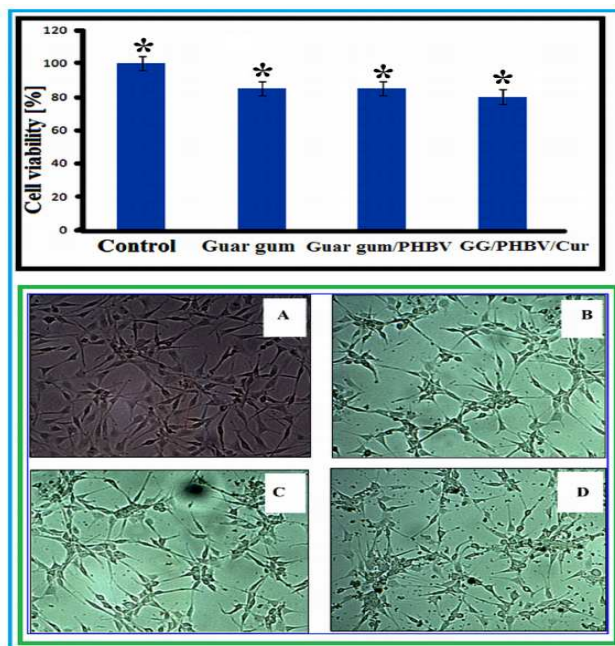


Figure 12: *In vitro* cytotoxicity and Cell proliferation studies (MTT assay) of A) Control, B) Guar gum, C) Guar gum/ PHBV and D) Guar gum/ PHBV/curcumin blend film in NIH 3T3 fibroblast cell line. The values are shown as means and standard errors ($n=3$), $*p<0.05$ (significant). *denotes the significant change in comparison to the control.

Discussion

Figure 1 demonstrated the UV-visible absorbance spectra of PHBV/guar gum blend film in the wavelength range of 190-380 nm. The figure revealed that with the increasing content of PHBV in the blend films, the opacity of the films was increased [**Table 2**]. Pure guar gum film showed the maximum transparency than that of guar gum/PHBV blend films in the UV region. This may be due to the yielding of fine grained polycrystalline structure into guar gum/PHBV blend films. Again, the blend films were found to act as a barrier to block the UV-Visible rays at shorter ranges of wavelength (190-300 nm). Since, the most pronounced effect of light on wound spot is caused by the ultraviolet light,

therefore, it is concluded that the guar gum/PHBV blend films can be used to block the UV rays that may be beneficial for the inhibition of DNA rupture and dimerization of thymine molecules present in the wound^[31].

Mechanical Properties:

Table 1 revealed that with the increasing contents of PHBV, the tensile strength and the elongation at break (%) were increased initially than that of pure guar gum. For 7:3 guar gum/PHBV blend, the maximum tensile strength was observed to be 19.8 MPa. The high tensile strength values of these films could be attributed to the formation of intermolecular hydrogen bonding between -C=O group of the PHBV backbone and -OH group of the guar gum. Again, with the increasing content of PHBV (from 30% to 70%) in the blend films, the brittleness of the films was found to increase. Therefore, the tensile strength and the elongation at break (%) of the blend films were decreased significantly with the increasing content of PHBV in the blend.

Figure 2 displayed the coupling of bonded protons with neighbouring adjacent vicinal protons in curcumin, *C. longa*. The strong absorption peaks at 6.92 ppm (1H, d), 7.18 ppm (1H, dd) and 7.29 ppm (d, 1H,) indicated the presence of three substituted benzene protons. A low field shifted absorption peaks at 6.03 ppm (s, 2H) and 7.63 ppm (1H, d) assigned for the trans double bond while signal at 3.81 ppm (s, 3H) revealed the presence of phenolic methoxyl group in curcumin structure. The experimental outcome is in agreement with the report presented by Goren et al^[32].

The ^1H NMR spectrum of polyester indicated that methyl protons (-CH_3) of the HB side group had a doublet resonance

at 1.253 ppm and methyl protons (-CH_3) of HV side group at 0.878 ppm with triplet resonance, due to the coupling with the adjacent methylene group. A group of strong absorption peaks at 1.606 ppm, 2.307 ppm for ethylene protons (-CH_2) of HV side group and (-CH_2) of HV- HB bulk structure with multiple resonance indicated the splitting of adjacent methylene and methyl protons in the presence of external magnetic field. Again, the methine proton, -CH (HV and HB bulk structure) linked with more electronegative oxygen atom had a multiplet resonance with more downfield chemical shift value at 5.340 ppm due to the deshielding effect of methine proton.

Again, the $^1\text{HNMR}$ spectra of pure guar gum showed the absorption peaks at $\delta=4.67$ ppm (s) and $\delta=3.5\text{--}3.9$ ppm (m) which exhibited the presence of anomeric protons and the residual protons of mannose/galactose ring in guar gum. The chemical shift value at 5.02 ppm, 3.81 and 3.96 ppm indicated the presence of methane (-C-H) group and methylenes (-CH_2 group) at C_6 and C_6' point of galactopyranosyl structure in sugar unit.

The stretching frequency of different mode of vibration of curcumin, guar gum, PHBV and their blend was shown in **Figure 3**. In PHBV copolymer, a strong band at 1283 cm^{-1} was due to the presence of an ester bond in the copolymer. Methyl (-CH_3) group provided a peak at 1383 cm^{-1} whereas methylene (-CH_2) groups at 1449 cm^{-1} were due to the bending mode of vibration; methine (-CH) group at 2930 cm^{-1} was due to asymmetric stretching vibration. A peak of -C=O functional group at 1727 cm^{-1} and a strong absorption peak of a hydroxyl group (-OH) at 3429 cm^{-1} respectively confirmed

the chemical structure of copolymer. For the pure guar gum, the strong absorption band was observed at 3269 cm^{-1} due to the stretching vibration of $-\text{OH}$ group. The bands around 1162 cm^{-1} and 2926 cm^{-1} assigned to C-O bond stretching and C-H bond stretching and two strong bands around 1100 and 1024 cm^{-1} were due to the presence of C-O-C bond stretching. In pure curcumin, the stretching frequency at 3400 cm^{-1} revealed the strong absorption band of hydroxyl group ($-\text{OH}$). In case of enolic $-\text{OH}$ stretching, the vibration mode was observed at 2979 cm^{-1} . The peaks at 1376 cm^{-1} , 1483 cm^{-1} and 1625 cm^{-1} were assigned for the stretching of C=C (aromatic), C=C (olefinic) and C=O groups, respectively. Another significant absorption bands were observed around 725 and 814 cm^{-1} , assigned to the $-\text{C}=\text{C}-\text{H}$ aromatic bending mode of vibration.

FTIR spectra of the different guar gum/PHBV blend films exhibited the decreasing trends of stretching frequency (from 3267 cm^{-1} to nearly 3300 cm^{-1}) of $-\text{OH}$ group than that present in pure PHBV polymer. In **Figure 3**, it was observed that with the increasing contents of PHBV, the stretching frequencies were increased from 3267 cm^{-1} to 3320 cm^{-1} , whereas the $-\text{OH}$ stretching of pure guar gum was observed at 3251 cm^{-1} . Again, for pure PHBV, the $-\text{OH}$ group stretching frequency was found around 3400 cm^{-1} but in case of guar gum/PHBV blend, the absorption peaks were shifted to lower ranges of frequency (3267 cm^{-1} , 3286 cm^{-1} and 3320 cm^{-1}) as shown in **ESI 1-Table 3 and Figure 3**. The decreasing trend of stretching frequency of hydroxyl group ($-\text{OH}$) and carbonyl group ($-\text{C}=\text{O}$) of the blend was probably due to the breaking of intra and inter-molecular hydrogen bonding in guar gum

structure and consequent re-formation of the intermolecular hydrogen bonding between the hydroxyl group of guar gum and carbonyl group of PHBV copolymer. Therefore, PHBV biopolymer may intercalate in between the pyranose rings of guar gum units and bound itself through the non-covalent interaction (H-bonding or hydrophobic-hydrophobic interaction) with functional groups of guar gum molecules.

Thermo-gravimetric analysis (TGA):

Pure guar gum showed poor thermal stability which was found to improve on its blending with PHBV as shown in **Figure 4**. The effects of thermal degradation were weakened when the PHBV content in the blends was decreased. The results showed that the degradation occurred in two steps. The first step in degradation between $60-100^\circ\text{C}$ was due to the evaporation of weakly bonded water molecules whereas in the second step ($150-330^\circ\text{C}$), the peaks appeared due to the degradation of samples. For both of guar gum and PHBV, the weight loss started at 120°C and the weight loss was found to be at 52% and 33%, respectively at 250°C as shown in **Table 4**. Again, the blends of guar gum and PHBV, showed two different steps: one at $250-280^\circ\text{C}$ and the other one at around $354-400^\circ\text{C}$. The first peak can be assigned to the decomposition of guar gum and the second one is related to the decomposition of PHBV derivatives. The maximum degradation rate was slightly shifted to lower values [68%, 62% and 33%] with the increase in the PHBV content in the blend. Again, from the DSC diagram, it was observed that the melting temperature of the blend shifted to higher values than that of pure PHBV biopolymer. This may be due to the intermolecular interaction between PHBV and the highly

rigid guar gum molecules surrounding the PHBV molecules to make the PHBV molecules flexible in the blends^[33].

Atomic force microscopic (AFM) study:

Surface morphology of guar gum and PHBV-guar gum blend films displayed the regularities of each component in the composition. It can be seen from **Figure 5** that the film of pure guar showed a uniform characteristic ridge and valley structure. The surface smoothness was differed to some extent when the PHA contents in the blends were increased and the blend film showed more irregularities with uneven surfaces. The surface of guar gum/PHBV blend is more or less uniform, which may be attributed to the high concentration of PHBV in the blend films. It may also be due to the insufficient coverage of PHBV chains on membrane surface. Therefore, the roughness parameter (RMS value) of the guar-PHBV blend films was found to increase compared to unmodified films. Since, in biomedical field, the nanoscale roughness plays a vital role on cell proliferation, therefore, it will be beneficial for their biomedical applications.

Again, the nanoscale or microscale surface roughness, which directly corresponds to the sizes of proteins and cell membrane receptors, could also play an important role in osteoblast differentiation and tissue regeneration^[34, 35]. Therefore, increase of roughness values in the blend composition may be opted for the cell proliferation onto the wound.

Swelling studies

Initially, PHBV copolymer did not show any solubility or swelling in water due to its hydrophobic character. When, the guar gum content was increased from 30 to 70 wt%, swelling of the blended films was found to increase as shown in **Figure 6**. Physical integrity of the blended films was maintained even though the blended films were incubated for 24 hours. The enhanced swelling could arise from the intra or intermolecular network in the polymer film. Again, swelling is one of the important criteria which determine the usefulness of the material in the artificial skin and wound dressing applications^[15]. In the presence of 70% guar gum, the water absorption capacity of the blended film was found to increase up to 400-470%. Therefore, the presence of guar gum in the blend may affect on the water uptake capacity; this may be due to the presence of free hydrophilic groups and free volume in the blend films.

Furthermore, the water uptake is also affected by the hydrogen bond formation and crystallinity of copolymer content^[26]. Guar gum/PHBV blend film with 70% guar gum showed highest hydrophilicity because it had more hydroxyl groups and less crystalline than that of the other blended films. Therefore, this 70:30 guar gum/PHBV blend film with good hydrophilicity may be favorable one for testing of cell adhesion and proliferation^[20] compared to the pure PHBV.

Etching phenomena of the composite films showed that with the increasing contents of PHBV, the degradation of the surface was facilitated [**Figure 7**]. Chloroform is used the etching agent as it can dissolve the PHBV biopolymer from the blend. Again, the results revealed that with the increasing

contents of PHBV in the blend film, the smoothness of the surface was diminished in etching condition and formed deep pit like 3D scaffold. Therefore, it is concluded that the blending components, guar gum and PHBV biopolymer were uniformly distributed throughout the blends.

BSA adsorption on the polymer surfaces depends on the protein concentration, adsorption time and nature of the polymer surfaces. The adsorption results showed that with the increase in hydrophobicity, the binding of protein molecules was facilitated and the maximum protein adsorption was found to be 70% for guar gum/PHBV/curcumin blend film having 30% of PHBV content. Again, the ATR spectra [Figure 8] of BSA adsorbed blend films indicated the corresponding stretching frequency at 3400 cm^{-1} (amide A) for N-H stretching vibration, 3100 cm^{-1} (amide A), in between $1600\text{--}1700\text{ cm}^{-1}$ (amide I) for C=O group and 1510 and 1580 cm^{-1} region (amide II) for in plane bending of N-H group. These spectral evidences reinforced the protein adsorption on the polymer surfaces. Since, protein adsorption is an indicator about the adherence of the cell on the polymeric surfaces, our results indicated that curcumin loaded 7:3 guar gum/PHBV film could adhere cells in a better way^[36].

Hemolytic assays:

Hemolytic assays of biomaterials with human blood having significant compatibility not only concern the platelet adhesion and activation, but also involve the hemolysis of red blood cells (RBC). Significant value of hemolysis less than 4% indicates the prevention of RBC from damage by the guar gum/PHBV/curcumin sample in contact of human blood

[Figure 9]. Therefore, the lower value of hemolysis (%) of acceptable biomaterials is suitable for wound healing applications^[37]. The protected RBC can be significantly worked out for the deformation and expose of procoagulant phospholipids (phosphatidyl serine) on the film surface. It is similar to the activated platelets through the assembly of prothrombinase complexes that catalyzes the conversion of prothrombin to thrombin in the maturation stage of healing^[38].

Antimicrobial activity:

Bactericidal phenomenon of curcumin and curcumin loaded films was quantified by the measurement of zone-inhibition. The antibacterial activity of all the specimens was demonstrated in Figure 10. From the images, it can be seen that pure guar gum and guar gum/PHBV blend film [used as a control] exhibited no significant bactericidal activity whereas curcumin and guar gum/PHBV/curcumin blend film significantly prevented the cell growth of bacterial strains. The profound antibacterial activity was observed against gram-positive strains than that of gram negative strains. The genes FtsZ (a prokaryotic cytoskeletal element) present in bacterial genome is responsible for the cell viability and cell proliferation^[39]. Curcumin can reduce the bundling of FtsZ protofilaments in the Z-ring, leading to suppression of bacterial proliferation which in turn can result in anti-bacterial activity^[40]. From this figure, it can be concluded that both curcumin and curcumin loaded films are able to suppress the growth of bacterial strains.

Curcumin release

The *invitro* curcumin release from guar gum/PHBV blend film was monitored for a period of 36 hours as shown in **Figure 11**. Curcumin was found to release slowly at a constant rate throughout the period of release. The initial burst release of 80% of curcumin from guar gum film was occurred within the period of 18 hours but the rate of burst release was significantly reduced for other delivery systems. The lower rate of release could be due to the incorporation of curcumin within the hydrophobic cavity of the polymer networks. Meanwhile, the blended composition of guar gum/PHBV (7:3) showed sustain release (35%) of curcumin on 18 hours of incubation. Again, with the increasing contents of PHBV, the release of curcumin was found to decrease. Since, PHBV is a slow degrading polymer and degrades via surface erosion, therefore, low burst release of drug may be due to the enhanced hydrophobic environment of PHBV units in the blend films. In the present study, the curcumin release profiles [**Figure 11**] are consistent with the change of the hydrophobicity of the film, indicating the possibility of controlling the rate of curcumin release from the film by modifying the material surface with semicrystalline hydrophobic structure. Again, curcumin mainly contains hydrophobic aromatic compound and it is unlikely to be bounded/encapsulated by a hydrophilic polymer such as guar gum, whereas the presence of PHBV, a hydrophobic polymer, in the blend enhances its capability to encapsulate curcumin through hydrophobic-hydrophobic interaction. Moreover, comparing the rate of curcumin release, it seems that curcumin within high hydrophobic environment is more

likely to be retained in the hydrophobic network. This behavior controls the burst release of hydrophobic drugs.

Cell viability:

In order to investigate the cytotoxicity of the curcumin loaded film, the evaluation on the cell viability was conducted for the potential use of the films as a wound dressing materials [**Figure 12**]. It is well known that the cytotoxic effects of curcumin depend on the dose and the type of cell line. Since, the surface roughness of the blend film may affect the cell growth to some extent as the number of metabolically active cell is dependent on the surface property of the polymer blends for their adherence. The number of cells adhering to the polymeric film was nearly similar on both 7:3 guar gum/PHBV and curcumin loaded guar gum/PHBV blend films. Therefore, no obvious differences in cell morphology were observed among the cells grown on guar gum films with its PHBV composite and none of the three surfaces (guar gum, guar gum/PHBV and guar gum/PHBV/curcumin) had elicited any major deleterious or cytotoxic responses of the cells. Therefore, guar gum/PHBV/curcumin composite is suitable for fibroblast cell adhesion as well as cell proliferation. It may be attributed to the hydrophilic-hydrophobic networking system responsible for the support of fibroblast cell viability and proliferation more than that of polymer surface of pure guar gum^[24]. Therefore, fibroblast cell is significantly biocompatible to the polymer composites.

Animal study:

In the present study, the positive impact on the wound healing of skin was observed by curcumin loaded film than the control experiment. After 7 days of experiment on wound

healing, it was observed that the curcumin loaded film enhanced the cure process with nearly 90% of wound contraction through cell proliferation and maturation significantly as shown in **ESI 2-Figure 13**. But in case of control experiment, the wound area seems to scar formation with only 55% of wound contraction. Curcumin is well known for its antioxidant activity and improving collagen content in the wound on skin ^[41].

The improvement of wound healing process in case of test sample may be due to the alignment of curing process by curcumin loaded films. Experimental report revealed that curcumin improved the wounded skin by an increase in fibroblast content and vascular density in wounds and prevent oxidative damage on skin ^[42]. The curcumin was found to increase the content of collagen, hexamine, uronic acid and DNA which assisted the wound healing faster without any scar formation compared to the control experiment ^[43]. The concentration of curcumin is another factor for wound healing. Faster release of curcumin may increase its concentration on the wound within a short period. This can be overweighed to cause cytotoxicity on the wound. In the present study, the guar gum/PHBV/curcumin film controls the release of curcumin to reinforce the healing process. There are several guar gum/PHBV ratios which are responsible to control the release rate but 7:3 guar gum/PHBV blends was found to be a suitable vehicle for the sustainable release of curcumin with maximum improvement in wound healing. The result was consistent with MTT assays and hemolytic assays in which the guar gum/PHBV/curcumin blend film significantly improved the cell viability, cell adhesion and

cell proliferation that supported the wound healing. Therefore, guar gum/PHA/curcumin composite film having nanoscale surface roughness can be used as an alternative wound dressing materials.

Experimental section

Methods & Materials

Materials and Animals

Guar gum powder of endosperm and glycerol were purchased from Merck India, Ltd. 3-[4, 5-dimethylthiazol-2-yl]-2, 5-diphenyltetrazolium bromide (MTT) were purchased from Sigma-Aldrich. *Curcuma longa* (turmeric) was collected from local area of Mamabhagina (Bagdah), District-North 24 Parganas, West Bengal, India. All solvents/chemicals used were of AR/HPLC grade and obtained from SRL.

Male Swiss-albino mice (n=6) weighing 32-34±2g was collected from the Animal Centre of Calcutta University. The mice were housed singly to prevent fighting and attack on the wounds and received food and water. All the animals would be in quarantine for a week before treatment. All animal experiment procedures were performed following the protocol approved by the animal ethical committee, Department of Physiology, University of Calcutta, in accordance with the guideline of the committee for the purpose of control and supervision of experiments on animal (CPCSEA Ref no: 820/04/ac/CPCSEA dated 06.08.2004), Government of India.

Microorganisms

The bacterial strain used to extract biopolymer, poly(3hydroxybutyrate-co-3hydroxyvalerate) [PHBV] copolymer was *Alkaliphilus oremlandii* ohILAs strain. The

detail of the polymer extraction had been described in our previous report ^[3].

Extraction of Curcumin

100g of dried turmeric was first grinded in a mixer grinder. It was air dried to remove the moisture present in the ground turmeric powder at 50°C in a hot air oven for six hours. Then, 10g of dried turmeric powder was washed with de-ionized water, sliced and dried in the sun for one week. The dried turmeric powder was then placed in a timber of soxhlet extractor. It was set up with various solvents from non polar to polar [acetone (B.P. =56.53°C), chloroform (B.P. =61°C) and methanol (B.P. =65°C)]. 50 ml of each solvent was added and extracted according to their boiling point for six hours. The reflux was carried out sequentially for six to seven hours to ensure the complete extraction of curcumin. Then, the paste of turmeric oil was evaporated to dryness at 40°C to obtain the pure orange-yellow crystal of curcuminoids. In final step, pure curcumin powder was extracted by using Column chromatography in silica gel glass column and the fine crystals were measured to calculate the yield of curcuminoids. The proton environment of the pure curcumin was analyzed in CDCl₃ solution using a JEOL ALPHA -400 spectrometer.

Purification of guar gum molecules

The purification of guar-gum was carried out based on the procedure described by Adriana ^[44] et al. Approximately 3g of the guar gum was solubilized in 100 ml of de-ionized water

at 30°C with the constant stirring at 105 rpm for 24 hours. Then the sample was centrifuged at 4000 rpm for 25 minutes to remove the insoluble materials. The supernatant was precipitated into an equal volume of 25 ml of 80% (v/v) ethanol. The precipitate was collected on a glass filter and washed successively with ethanol and acetone, and then it was dried with hot air.

Preparation of curcumin (drug) loaded P(3HB-co-3HB)/guar gum blend films

The di-polymeric blend film was prepared by solvent casting method. A series of blends were prepared with varying concentrations of P(3HB-co-3HV) copolymer and guar gum. Purified guar gum powder in different weight percentages (30, 50, and 70 wt%) were dissolved in 30 ml of double distilled water by the stirring at 60°C for 90 min until a clear solution was appeared and it was then cooled at room temperature. P(3HB-co-4HB)[PHBV] copolymer [70, 50 and 30 wt%] was also dissolved in 30 ml of chloroform solution. The purified curcumin (40 mg) was also dissolved in 10 ml of chloroform solution and then both solutions were mixed with the guar gum solution. The mixture was stirred overnight to obtain a homogenous solution. Finally, the mixed solution was poured on Teflon plates (12 cm × 12 cm) resting on an even- leveled surface, forming film by using solvent casting method and dried at room temperature for 24 hrs at 40°C until the solvents were completely evaporated.

The thickness of the blend films was determined by using a dial thickness gauge micrometer (Mitutoyo Manufacturing

Co. Ltd., Japan) at six random positions on the films and the mean thickness was calculated.

The mechanical properties [tensile strength, Young's modulus] of the films [$50 \times 25 \text{ mm}^2$] were measured by using a texture analyzer (TA. XT Plus, Texture Technologies, USA) equipped with a 5 kg load cell at a rate of 50 mm/min until breaking.

Optical properties

The light transmittance capacity of the blend film was measured by the absorption of light directly in a spectrophotometer test cell (Optizen view, Mecasys, Korea) in the wavelength range from 200 nm to 800 nm at a resolution of 1 nm. The specimens were first cut in rectangular shape and measurements were performed using air as the reference. Each sample was measured in triplicate and the average of these values was calculated. The transparency at 600 nm (T_{600}) was obtained from the following equation described by Han and Floros^[45] et al. (1997):

$$T_{600} = \log T (\%) / b \dots \dots \dots (1)$$

Where T is percentage transmittance (%) and b is the thickness (mm) of the specimen film. Finally, the opacity of the films was calculated by using the following equation described by Gontard et al^[46]:

$$\text{Opacity} = \text{absorbance at } 500 \text{ nm} \times \text{film thickness} \dots \dots \dots (2)$$

Swelling study

The swelling behavior of the films was monitored by the swelling of specimens in phosphate buffer saline solution (pH 7.4) at 37°C. The pre-weighed dry films [guar gum/PHBV blend films] were then immersed in 10 ml of phosphate buffers (pH 7.4) solution at 37°C and the films were withdrawn at definite time interval [initially 30 minutes and then 1 hour time interval] for 24 hours. Then, the weight of the swollen films was measured after wiping out the liquid with blotting paper. The swelling percentage was calculated as follows:

$$\text{Swelling (\%), } Q = (\text{Weight of the swollen films} / \text{Weight of the dry films}) \times 100 \dots \dots \dots (3)$$

The experimental results (data) are an average of triplicate values of each reading.

Protein adsorption

The surface adsorptions of protein on the surface of blend films [pure guar gum, guar gum/PHBV and guar gum/PHBV/curcumin] were investigated by incubating the films separately in 5 ml (2mg/ml) of bovine serum albumin (BSA) solution for 24 hours at 37°C. About 300µl of protein solution was withdrawn from the sample solution within a definite time interval and the change of concentration of solution was recorded by using a UV-Visible spectrophotometer at 280 nm. Again, the adsorbed proteins on the surface of the polymer films were analyzed by ATR-FTIR (model-Alpha, Bruker, Germany) spectrometer,

scanning from 4000 cm^{-1} to 550 cm^{-1} for 42 consecutive scans at room temperature.

Etching of different composite films

To investigate about the surface-morphology of the blend composition and also about the nature of dispersion of the two polymeric components in the film, the etching tests of the blended films were performed in chloroform solvent. The specimen of different films was cut into pieces and it was dipped in chloroform solvent at 30°C for 24 hours with constant stirring at 105 rpm. Then, the etched samples were oven dried at 40°C for 6 hours and kept in a desiccator for spectroscopic analysis [scanning electron microscope (Model: Philips XL30, Carl Zeiss, Germany)] after coating the sample with gold under vacuum.

Hemolytic assay

5 ml of fresh human blood was collected in a heparinized-tube in the absence of any anticoagulant. Then, the coagulated blood was centrifuged at 1500 rpm for 20 min at 4°C to obtain the serum. After the supernatant plasma was discarded, the erythrocytes (RBC) were washed three times with physiological saline, Phosphate Buffer Saline (PBS) in order to remove serum proteins. After the final washing step, the final erythrocytes were dispersed in normal physiological saline to obtain an erythrocyte suspension. The different volume of samples in tubes (10, 20, 30, 40, 50, 100 μl) having a concentration of 1mg/ml were taken and made up to 950 μl with PBS solution, followed by the addition and mixing of 50 μl of RBC sample. For positive control and negative control

tests, 950 μl of sterilized de-ionized water and 950 μl of PBS solutions were mixed with the sample solutions. Finally, all stocks were incubated in dark condition for 10 minutes and then centrifuged for 10 minutes at 6,000 rpm at 4°C. The absorbance values (A) of supernatants were determined at 540 nm by a spectrophotometer. Finally, the percentage of hemolysis was calculated by using the formula given below-

$$\text{Percentage of hemolysis} = \frac{(A_{\text{sample}} - A_{\text{negative control}})}{(A_{\text{positive control}} - A_{\text{negative control}})} \times 100 \% \dots \dots \dots (4)$$

[Hemolytic condition: >5% of hemolysis]

Antimicrobial activity of pure curcumin and curcumin loaded film:

The antimicrobial properties of the extracted pure curcumin and curcumin loaded guar gum/PHBV films were tested by using agar well-diffusion and disc diffusion method against several bacterial cultures, namely, *E.coli* XL1B, *Staphylococcus aureus*, *Enterobacter aerogenes*, *Vibrio vulnificus*, *Bacillus subtilis* and *Pseudomonas aeruginosa* strain. For disc diffusion method, the films were cut into a disc shape with 4 mm diameter, sterilized by autoclaving for 15 minutes at 121°C under 15 psi pressure. Again, for well-diffusion method, the concentrated DMSO solution of curcumin (4mg) was placed into the well of the culture agar plates. The plates were incubated for 24 hours at 37°C in an incubation chamber and the inhibition zone was then measured.

***In vitro* curcumin (drug) release study**

To investigate, the release kinetics of curcumin from the curcumin loaded films, 0.065g [25 mm²] of each film was placed in a vial filled with a 10 ml of phosphate buffer solution (pH 7.4) at room temperature. The amount of curcumin released at different time intervals (0, 2, 4, 6, 12, 24 and 36 hours) was recorded by using the UV-Visible spectrophotometer [(Optizen view, Mecasys, Korea)] at a resolution of 1 nm at a fixed wavelength of 425 nm. The recorded absorbance was then related to the amount of released curcumin using a calibration plot according to the previous reports [47, 48]. The percentage of curcumin released in the consecutive time -intervals was quantified as follows:

$$\text{Percentage of curcumin release} = (\text{Released curcumin} / \text{Total curcumin}) \times 100 \dots \dots \dots (5)$$

In vitro* cell line study*Cell proliferation studies**

For cytotoxicity experiments, Cells were grown in DMEM (Dulbecco's modified Eagle's medium) supplemented with 10% (v/v) fetal bovine serum and 1% antibiotic and were incubated at 37°C in 5% CO₂ humidified atmosphere. 96 well culture plates made of polystyrene (Tarson, India) were coated with different concentrated (1, 2, 3, 4 and 5 mg/ml) solution of guar gum, PHBV/guar gum and curcumin loaded PHBV/guar gum blend. The plates were dried in a laminar air flow hood followed by the UV-rays sterilization. The cells were seeded at the density of 0.5×10⁶ per well and incubated at 37°C in a humidified atmosphere containing 5% CO₂. After

12 h of incubation, the supernatant of each well was replaced with methyl thiazoyl tetrazolium bromide (MTT) diluted in serum-free medium and the plates were incubated at 37°C for 4 h. After removing the MTT solution, a mixture of acid and isopropanol (0.04 N HCl in isopropanol) was added to each well and pipetted up and down to dissolve all of the dark blue crystals and then left at room temperature for a few minutes to ensure the dissolution of all crystals. Finally, absorbance was measured at 570 nm using a UV spectrophotometer. Each experiment was performed at least three times. The sets of three wells for the MTT assay were used and their average was taken as the final result. Cell viability was expressed as the percentage of the negative control calculated as

$$\text{Cell viability (\%)} = (N_t / N_c) \times 100 \dots \dots \dots (6)$$

Where N_t and N_c are the optical density of treated cells and untreated cell respectively.

Wound healing assay in animal model

Male mice were housed under standard conditions with a controlled temperature of 25°C and a light/dark cycle of 12/12 h. The wound on the thigh were created by cutting certain area (4mm×5mm) of skin before hairs on the skin were completely removed using hair removal cream. Then, the wound areas were sterilized using povidone iodine. The wound area then uniformly dressed with 5mm×6mm size of the test sample [guar gum/PHBV/curcumin loaded films, size] and also covered with commercial gauze. Routinely the wound had been examined and the position of the test sample was monitored. The test sample was also placed onto the wound properly and regularly monitored to check if any

displaced of the test samples have occurred or not due to the activity of the mice. Again, wound area of control mice was simply covered with commercial gauze. The wound contraction areas of the control and test mice (treated with guar gum/PHBV/curcumin loaded films) were recorded by scaling with transparent tape for 0 day, 2 days, 4 days and 7 days.

Characterization

UV-Visible spectra analysis

The light absorption capacity of the pure guar gum film and its guar gum/PHBV blend film was recorded by using UV-Visible spectrophotometer ((Optizen view, Mecasys) at a resolution of 1 nm.

FTIR spectral analysis:

Fourier Transform Infrared (FTIR) spectroscopic characterization of samples was carried out with ATR- FTIR (model-Alpha, Bruker, Germany) spectrometer, scanning from 4000 cm^{-1} to 550 cm^{-1} for 42 consecutive scans at room temperature. The stretching frequency of each functional groups [C-H, C-C, C-O, C=O] was recorded with FTIR spectrum. Each of polyester (1mg) was mixed with 25 mg of KBr to form KBr plate for the IR analysis at room temperature.

^1H NMR spectral analysis:

The chemical structure of the copolymer [P(3-HB-co-3-HV)], guar gum and extracted curcumin were confirmed by measuring the chemical shift position in ^1H NMR spectroscopy. The analysis of the sample was carried out on a

JEOL ALPHA -400 spectrometer at 25°C . Tetramethylsilane was used an internal chemical shift standard.

Thermogravimetric analysis (TGA)

Thermogravimetric analysis (TGA) of guar gum and guar gum/PHBV blend samples was carried out on a Q50 (V20.6 build 31) TGA (TA instruments, USA) at a heating rate of $10^\circ\text{C}/\text{min}$ from 30 to 600°C in nitrogen flow.

Atomic force Microscopic Analysis

The surface morphology of the samples was determined by using atomic force microscope (AFM) [AFM (VEECO, Multimode Nanoscope IIIa)] operating in the tapping mode (RTESP Tip with resonant frequency 301.78 KHz) at room temperature.

Scanning electron microscopic (SEM) analysis

The morphology of pure guar gum film and guar gum/PHBV films were investigated using a scanning electron microscope (Model: Philips XL30, Carl Zeiss, Germany) after coating the sample with gold under vacuum.

Statistical analysis: All experiments were done in triplicates and reported values were the means of triplicate counts \pm standard deviations (SD).

Conclusion:

In the present study, we demonstrated that guar-gum/PHBV/curcumin blend film is able to accelerate the wound healing process. Characterization of the blend film by

ATR-FTIR, TGA and AFM indicated that these components were successfully blended by non-covalent interaction and their tensile strength was improved to a certain extent, making them suitable for clinical wound healing applications. In summary, the resultant blend exhibits thermal and mechanical endurance and physical characteristics in terms of swelling ratio and cell adhesion, making them ideal and versatile wound dressing materials for tissue construction and potential wound healing. This in fact was tested in animal models by curing the wound on the skin of animal using these curcumin loaded film made of a blend of guar gum and PHBV.

Acknowledgements

The authors gratefully acknowledge Technical Education Quality Improvement Programme (TEQIP) and CSIR grant-in-aid [No.02 (0008)/11/EMR-II], Government of India for their financial support in this experimental work. Again, all authors acknowledge Sourav Chakraborty (Operator, AFM) for their technical help in experimental analyses.

Conflict of Interest: No conflict of interest declared.

Notes and references

¹Advanced Polymer Laboratory, Department of Polymer Science & Technology, University of Calcutta, Kolkata-700009 (India), India,

²Central Leather Research Institute, Department of Biological Science (CLRI), Chennai, India,

³Department of Chemical Engineering, University of Calcutta, Kolkata-700009 (India), India

*Corresponding author, **E mail:** ppk923@yahoo.com;

Phone and fax: 91-33-2352-5106).

† Electronic Supplementary Information (ESI) available: ESI 1: Table 3 FTIR and ¹H NMR Spectra of guar gum, poly(3hydroxybutyrate-co-3hydroxyvalerate)(PHBV), Curcumin and their composite films; ESI 2: Figure 13 Photographs of macroscopic appearance of wound repair covered with (a) control, (b) curcumin composite films at day 0, day 2, day 4 and day 7 respectively.

See DOI: 10.1039/x0xx00000x

References

1. H. Brandl, R. Bachofen, J. Mayer and E. Wintermantel, *Can. J. Microbiol.*, 1995, **41**, 143–153.
2. H. Brandl, R. A. Gross, R.W. Lenz and R.C. Fuller, *Adv. Biochem. Eng. Biotechnol.*, 1990, **41**, 77–93.
3. N. Pramanik, K. Mukherjee, A. Nandy, S. Mukherjee and P. P. Kundu, *J. Appl. Polym. Sci.* 2014, **131**, 41080.
4. A. Steinbüchel, *Curr Opin Biotechnol*, 2005, **16**, 607–13.
5. A. Akar, E. U. Akkaya, S.K. Yesiladali, G. Celikyilmaz, E.U. Cokgor and C. Tamerler, *J Ind Microbiol Biotech.*, 2006, **33**, 215–20.
6. K. Zhao, Y. Deng, J. C. Chen and G. Q. Chen, *Biomaterials*, 2003, **24**, 1041–1045.
7. S. Philip, T. Keshavarz and I. Roy, *J Chem Technol Biotechnol.*, 2007, **82**, 233–247.
8. G. Q. Chena and Q. Wua, *Biomaterials*, 2005, **26**, 6565–6578.
9. C. W. Pouton and S. Akhtarb, *Advanced Drug Delivery Reviews*, 1996, **18**, 133-162.

ARTICLE

Journal Name

10. K. Rezwana, Q. Z. Chena, J.J. Blakera and A. R. T. Kiyosawa, Y. Sato and M. Ishihara, *Biomaterials*, 2010, **31**, 83–90.
11. D. P. Martin and S. F. Williams, *Biochem Eng J*, 2003, **3738**, 1–9.
12. B. Nebe, C. Forster, H. Pommerenke, G. Fulda, D. Behrend, U. Bernewski, K. P. Schmitz and J. Rychly, *Biomaterials*, 2001, **22(17)**, 2425–34.
13. B. Rihova, *Advanced Drug Delivery Reviews*, 2000, **42**, 65–80.
14. R. N. Reusch, *Can J Microbiol.*, 1995, **41(Suppl. 1)**, 50–4.
15. G. Peschel, H. M. Dahse, A. Konrad, G. D. Wieland, P. J. Mueller, D. P. Martin and M. Roth, *Journal of Biomedical Materials Research Part A*, 2008, **85(4)**, 1072–81.
16. Y. Doi, S. Kitamura and H. Abe, *Macromolecules*, 1995, **28**, 4822–8.
17. A. Sh. Asran, K. Razghandi, N. Aggarwal, G. H. Michler and T. Groth, *Biomacromolecules*, 2010, **11**, 3413–3421.
18. V. V. Terskiih and A. V. Vasiliev, *Int Rev Cytol.*, 1999, **188**, 41–72.
19. J. S. Boateng, K. H. Matthews, H. N. E. Stevens and Gillian M. Eccleston, *Journal of Pharmaceutical Sciences*, 2008, Vol. **97**, no. 8, 2892–2923.
20. J. Ostwald, S. Dommerich, C. Nischan and B. Kramp, *Laryngo Rhino Otol.*, 2003, **82**, 693–699.
21. S. Godbole, S. Gote, M. Latkar and T. Chakrabarti, *Bioresour. Technology*, 2003, **86**, 33–3.
22. K.W. Ng, H. L. Khor and D. W. Hutmacher, *Biomaterials*, 2004, **25**, 2807–2818.
23. K. Murakami, H. Aoki, S. Nakamura, S. Nakamura, M. Takikawa, M. Hanzawa, S. Kishimoto, H. Hattori, Y. Tanaka, N. R. Kil'deeva, G. A. Vikhoreva, L. S. Gal'braikh, A. V. Mironov, G. A. Bonartseva, P. A. Perminov, and A. N. Romashova, *Applied Biochemistry and Microbiology*, 2006, Vol. **42**, No. 6, pp. 631–635.
24. N. R. Kil'deeva, G. A. Vikhoreva, L. S. Gal'braikh, A. V. Mironov, G. A. Bonartseva, P. A. Perminov, and A. N. Romashova, *Applied Biochemistry and Microbiology*, 2006, Vol. **42**, No. 6, pp. 631–635.
25. C. Zhijianga, H. Chengweia and Y. Guanga, *Carbohydrate Polymers*, 2012, **87**, 1073–1080.
26. J. Kuang, K. Y. Yuk and K. M. Huh, *Carbohydrate Polymers*, 2011, **83**, 284–290.
27. Y. Huang, H. Yu and C. Xiao, *Carbohydrate Polymers*, 2007, **69**, 774–783.
28. F. Adriana, A. L. Rilton, D. Freitas, M. R. Sierakowski, N. Lucyszyn, G. L. Sasaki, B. M. Serafim and C. K. Saul, *Carbohydrate Polymers*, 2013, **93**, 484–491.
29. J. H. Han and J.D. Floros, *Journal of Plastic Film & Sheeting*, 1997, **13**, 287–298.
30. N. Gontard, and S. Guilbert, In M. Mathlouthi (Ed.), *Food packaging and preservation*, 1994, (pp. 159–181), New York: Blackie Academic & Professional.
31. S. Ekici and D. Saraydin, *Polym Int.*, 2007, **56**, 137.
32. P. L. Ritger and N.A. Peppas, *Control Release*, 1987, **5**, 37–42.
33. K. Varaprasad, Y. M. Mohan, K. Vimala and K. M. Raju, *Journal of Applied Polymer Science*, 2011, Vol. **121**, 784–796.
34. F. Lotfipour, A. Nokhodchi, A. Saeedi, S. N. Sani, J. Sharbafi and M. R. Siahi-Shadbad, *IL Farmaco*, 2004, **59**, 819–25.

35. M. J. Parnham and H. Wetzig, *Chem Phys Lipids*, 1993, **64**, 263–74.
36. A.L. Simal and A.R. Martin, *J. Appl. Polym. Sci.*, 1998, **68**, 453–474.
37. J. L. Ravanat, T. Douki and J. Cadet, *Journal of Photochemistry and Photobiology B: Biology*, 2001, **63**, 88–102.
38. M. Holmberg, K. B. Stibius, N. B. Larsen and X. Hou, *J Mater Sci: Mater Med.*, 2008, **19**, 2179–2185.
39. T. Ikejima and Y. Inoue, *Carbohydrate Polymers*, 2000, **41**, 351–356.
40. D. L. Cochran, *J. Periodontol.*, 1999, **70(12)**, 1523–39.
41. A. C. Gören, S. Çıkrıkçı, M. Çergel and G. Bilisel, *Food Chemistry*, 2009, **113**, 1239–1242.
42. D. D. Deligianni, N. D. Katsala, P. G. Koutsoukos and Y. F. Missirlis, *Biomaterials*, 2001, **22**, 87–96.
43. M. Shih, M. D. Shau, M. Y. Chang, S. K. Chiou, J. K. Chang, J. Y. Cherng, *International Journal of Pharmaceutics*, 2006, **327**, 117–125.
44. S. Y. Ong, J. Wu, S. M. Moochhala, M. H. Tan and J. Lu, *Biomaterials*, 2008, **29**, 4323–4332.
45. D. Rai, J. K. Singh, N. Roy, and D. Panda, *Biochemical Journal*, 2008, vol. **410**, no. 1, pp. 147–155.
46. S. Kaur, N. H. Modi, D. Panda, and N. Roy, *European Journal of Medicinal Chemistry*, 2010, vol. **45**, no. 9, pp. 4209–4214.
47. M. Panchatcharan, *Mol.Cell Biochem*, 2006, **290**, 87.
48. L. Thangapazham, A. Sharma, and R.K. Maheshwari, *Adv Exp Med Biol.*, 2007, **595**, 343.

Graphical Abstract

Characterization and evaluation of curcumin loaded guar gum-polyhydroxyalkanoates blend film for wound healing application

Nilkamal Pramanik¹, Tapas Mitra¹, Moumita Khamrai¹, Aditi Bhattacharyya¹, Piyasi Mukhopadhyay¹, A. Gnanamani², Ranjan Kumar Basu³, Patit Paban Kundu^{1*}

